FIRST INTERNATIONAL SEMINAR

ON

DEEP AND HIGH STRESS MINING

6-8 NOVEMBER 2002

PERTH, AUSTRALIA

Loading System Stiffness —A Parameter to Evaluate Rockburst Potential

T. Wiles *Mine Modelling Pty Ltd, Australia*

Loading System Stiffness —A Parameter to Evaluate Rockburst Potential

T. Wiles *Mine Modelling Pty Ltd, Australia*

Abstract

The strong correlation observed between pillar bursts and the local energy release rate suggests that this parameter can be used to predict the potential for rockbursts. By calculating local energy release rate for a variety of mining layouts it is shown that, owing to strong dependence on the local stress level, erroneous predictions can result, thus rendering this parameter unsuitable. However, if we normalise by the square of the mean stress, a representative measure of loading system stiffness can be obtained. This eliminates dependence on the local stress level and provides an indicator that can be used to predict more consistently the expected nature of failure independent of the local stress state.

1 Introduction

Elastic numerical modelling is often applied to predict rockmass response. It is generally well understood how the stress state (i.e. σ_1 versus σ_3 for the rockmass and τ versus σ_n for fault slip) can be used to predict when and where failure is expected. What is not clear is how to use elastic modelling predictions to predict the nature of these anticipated failures. It is highly desirable to identify locations where failures are expected to occur violently.

While 'controlled failures' are certainly of concern, since the resulting damage is driven by the advancing mining, damage can always be monitored and halted if necessary simply by suspending local mining activities. Remedial measures can be undertaken to ensure safety and limit production interruptions. By contrast, 'uncontrolled failures' that progress out of sequence with the advancing mining are of particular concern. To ensure safety, ground support measures must be taken prior to mining. If one could identify locations that were rockburst prone, special ground support measures could be taken in these areas and placed at an appropriate time in the mining sequence.

Previous efforts by the author (Wiles, 1998) have concentrated on the application of local energy release rate (LERR) calculations. Recent work has demonstrated that while this parameter correlates very well with observed bursting, it is not clear how to apply this technique to evaluate burst proneness.

2 Local energy release rate (LERR)

We begin by reviewing the theory behind energy release rate calculations. Consider a pillar between two drifts, and call 'Stage I' the model with the pillar intact. We now consider how the model responds if the pillar fails. In the model this is done by temporarily excavating the pillar (this assumes that the pillar will be obliterated during a rockburst); call this 'Stage II'. From these two stages, we can deduce certain characteristics of the loading system.

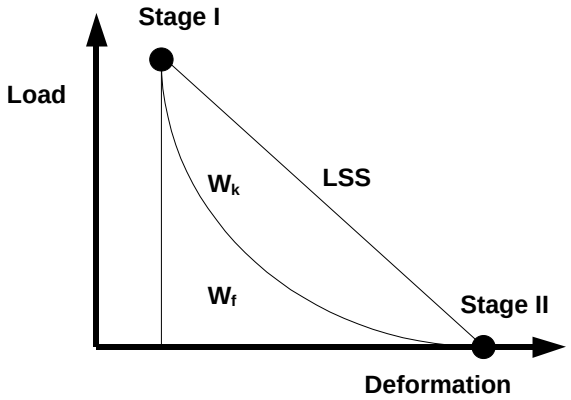

Figure 1 Load deformation response

The loading system stiffness (LSS) is simply the slope of the load deformation response curve.

The total amount of energy released from the surrounding rockmass during the pillar failure is the area of the triangle:

$$W_t = W_k + W_f \tag{1}$$

The amount of energy released as kinetic energy is the area of the upper portion of the triangle labelled as W_k. One should expect this to correlate with the observed event magnitude. The amount of energy that would be used in crushing the pillar is the area of the lower portion of the triangle labelled as W_f. One should expect this to correlate with the amount of damage observed at the event source.

The local energy release rate for this pillar is determined as:

$$\text{LERR} = W_t/\text{Volume} \tag{2}$$

It was shown in previous work (Wiles, 1998) that this parameter correlates very well with observed bursting. This was demonstrated by back analysing observed pillar bursts and showing that at the time of each burst, both the stress state (i.e. σ_1 versus σ_3) and LERR had consistent values at the burst location.

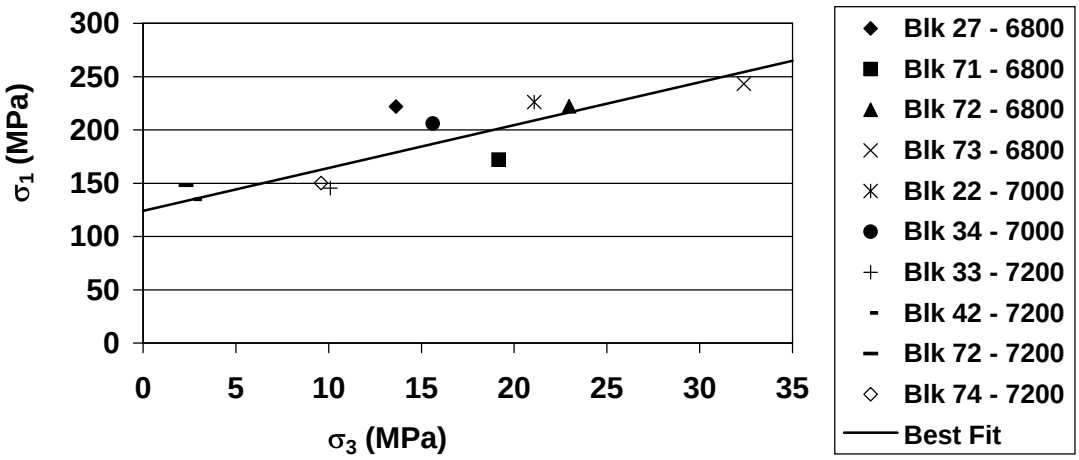

Figure 2 Stress state at time of burst

The stress state for each burst fits a linear strength criterion very well (Cv ≈ 9%).

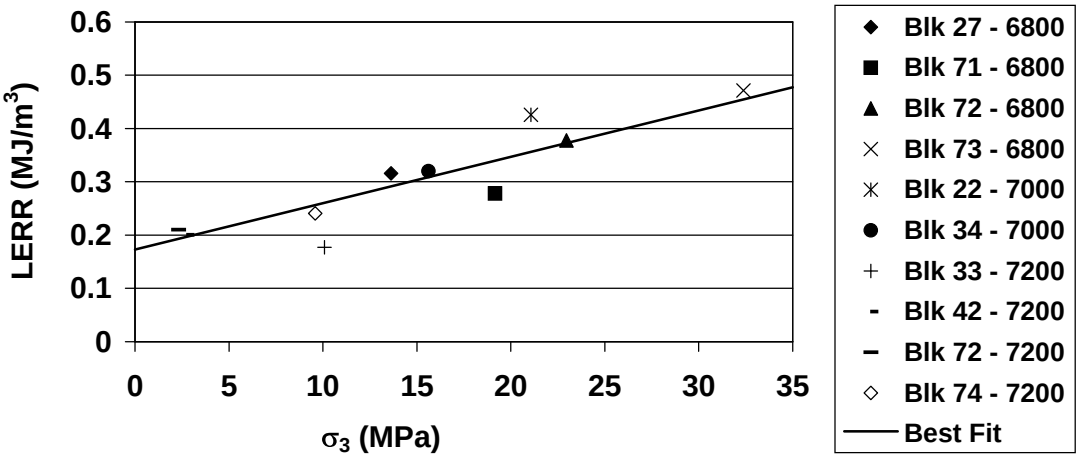

Figure 3 Local energy release rate at time of burst

The LERR for each burst also fits a linear criterion very well (Cv ≈ 14%).

In addition, it was shown that locations with insufficient LERR would fail without bursting and, certainly, that locations with insufficient stress would not fail at all.

3 The problem

It is desirable to apply this concept to evaluate burst potential. There are two separate issues here. First, we can determine the likelihood of failure by considering stress state (i.e. σ_1 versus σ_3).

Second, we can ask 'If a failure were to occur, would it be violent or not?'

Following from the Creighton back-analyses, it would seem relatively straightforward to simply calculate the LERR to make this evaluation. However, it will be shown below that it is not that simple. The problem is that this parameter is a strong function of the local stress level. Anywhere the stresses are high, so is LERR. Conversely, anywhere the stresses are low, so is LERR.

To demonstrate this problem, consider the simple example of a pillar between two drifts. Here the same model has been run but with different far field stress states.

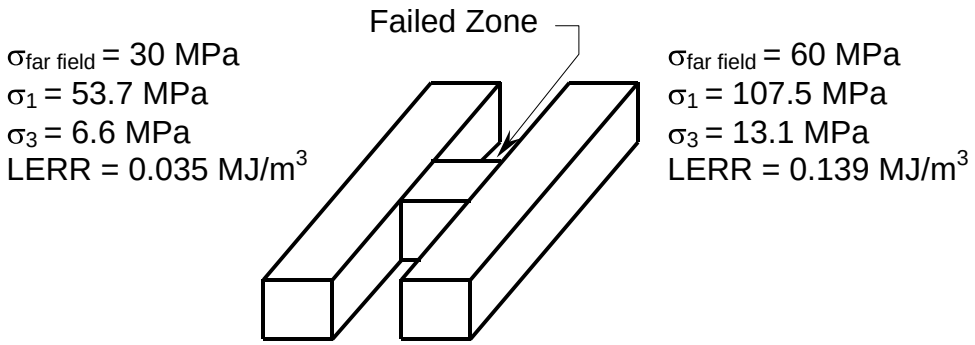

Figure 4 Pillar failure with different far field stress states

Although it is straightforward to determine the likelihood of failure from the stress state, if we now ask whether failure would be violent or not, the LERR concept cannot be applied, since the two models give very different values for LERR.

If we look closely at the mathematics behind the calculation, we will see that the magnitude varies as the square of the local stress level. Hence with double the stresses, LERR increases by a factor of four.

A second example considers the LERR adjacent to a large stope.

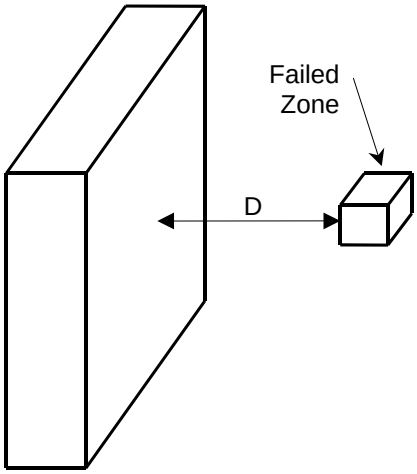

Figure 5 Failure near a large stope

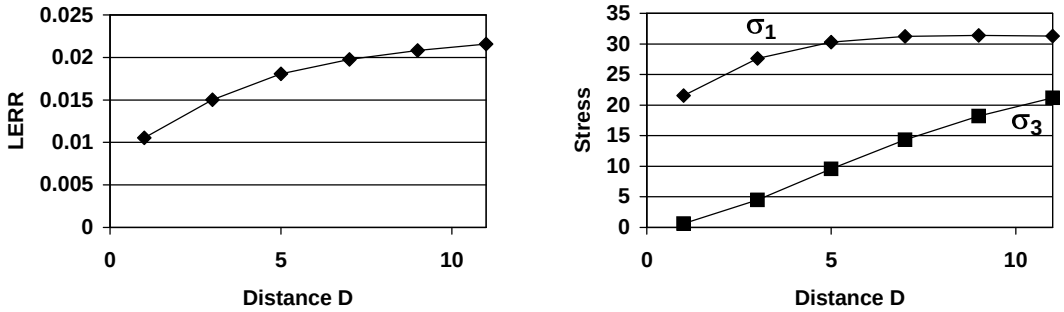

Figure 6 LERR and stresses near a large stope

Here we see that LERR actually increases as we move away from the stope. This incorrectly indicates that the rockburst potential is highest in the far field, and lowest adjacent to the mining. This erroneous result is due to the increasing stress level with distance from the stope. Separate from stress considerations, we would intuitively expect the burst potential to be worst in the immediate vicinity of the stope and diminish as we moved away.

Why are the back-analysis results from Creighton mine so consistent? The Creighton results show that when the stresses are exactly at the point of failure, the magnitude of LERR can be compared to determine burst potential. However, these simple examples demonstrate that when the stresses are not at the point of failure, the values of LERR cannot be used to determine burst potential. If we are to proceed, it would seem that some sort of normalisation is required to eliminate the dependence of LERR on stress level.

4 Loading system stiffness (LSS)

Now take a step back and review how LERR is calculated. The energy release rate concept originates in the fracture mechanics literature where Griffith (1921) showed that as a crack propagated, sufficient energy must be released from the rockmass to supply the energy requirements of forming the newly created crack surfaces. Later, Barenblatt (1962) showed that if an excess of energy was available, the crack would propagate unstably; it would spontaneously propagate without applying further loading.

It would appear that there is an obvious direct analogy to rockbursting, hence our consideration of LERR. However, there is a fundamental difference in the case of rockbursting. While in fracture propagation one is concerned with the rate of energy release as the crack increases in size, in the case of a pillar burst, we are interested in the rate of energy release as the non-linear strains accumulate. Thus the 'rate' that we are interested in is the amount of damage, rather than the changing extent of failure.

A measure of the rate of energy release as the non-linear strains accumulate is well encapsulated by considering loading system stiffness (LSS) rather than LERR. For a large value of LSS, energy is released relatively slowly with progressive damage, whereas with small values, energy is released at a much higher rate. The question of burst proneness now becomes a question of whether the failure occurs in a controlled manner, where all of the energy released can be used in accumulating damage (i.e. crushing of the pillar). Alternatively, the failure could occur in an uncontrolled manner, where there is more energy released than can be used in crushing of the pillar.

Returning for a moment to section 2, we determined from Figure 1 that the total energy released from the surrounding rockmass during pillar failure is the area of the triangle: $W_t = W_k + W_f$ (refer equation (1)). This is now readily calculated in a numerical model by integrating the forces through the displacements that occur from Stage I to Stage II, over all surfaces in the numerical model, thus:

$$W_t = \int\int (\sigma_n du_n + \sigma_s du_s + \sigma_t du_t) dS \tag{3}$$

Here, u represents the displacement, σ represents the surface stress, the subscripts n, s and t refer to the normal and two shear components on each surface S.

Unfortunately, the definition of LSS is not so straightforward. The LSS depicted in Figure 1 is for one direction on one surface only. There are different values in each direction (the normal and shear components) and different values for each surface in the model.

However, a representative LSS can be expressed in terms of the mean stress σ_m, and volumetric strain ε_v, by assuming that the pillar is filled with a fictitious material whose post-peak stiffness exactly matches the loading system response:

$$\sigma_m = \text{LSS}\ \varepsilon_v \tag{4}$$

Where:

$$\sigma_m = {}^1/_3(\sigma_1 + \sigma_2 + \sigma_3) \tag{5}$$

$$\varepsilon_v = \varepsilon_1 + \varepsilon_2 + \varepsilon_3 \tag{6}$$

We can calculate the strain energy of volume change as:

$$W_v = \int\int \sigma_m\, d\varepsilon_v\, dV \tag{7}$$

Where the volume integral is taken over the surfaces of the pillar that fails. Now substituting for the volumetric strain from Equation 4:

$$W_v = \int\int \sigma_m\, d\sigma_m\, dV/\,\text{LSS} \tag{8}$$

By equating this to the actual energy released from the loading system (W_t from Equation 3), we can determine the LSS for the fictitious material:

$$W_t \equiv W_v = \int\int \sigma_m\, d\sigma_m\, dV/\,\text{LSS} \tag{9}$$

and hence:

$$LSS = \int\int \sigma_m \, d\sigma_m \, dV / W_t \tag{10}$$

A closer look at the integral in this expression reveals that:

$$\int\int \sigma_m \, d\sigma_m \, dV = \tfrac{1}{2}\int \sigma_m^2 \, dV \approx \tfrac{1}{2} \, \overline{\sigma}_m^2 \, V \tag{11}$$

where $\overline{\sigma}_m^2$ represents the square of the average value of σ_m in the pillar with volume V.

An obvious question would be whether LSS defined as:

$$\sigma_m = LSS \, \varepsilon_v \tag{12}$$

has any special significance. Substituting Equation 11 into Equation 10 and inverting gives:

$$1/LSS = W_t / \int\int \sigma_m \, d\sigma_m \, dV \approx W_t / (\tfrac{1}{2} \, \overline{\sigma}_m^2 \, V) = 2 \, LERR / \overline{\sigma}_m^2 \tag{13}$$

which shows that calculation of LSS in this way is actually equivalent to normalising LERR by the square of the mean stress in the pillar.

5 Verification problems

5.1 Verification for spherical excavation

First consider a spherical excavation in a homogeneous stress field, far from all excavations. The radial deformation for such a shape is given by (Timoshenko and Goodier, 1934):

$$u = (1+\nu)pa/(2E) \tag{14}$$

Where p is the far field stress, a is the radius, E is Young's modulus and ν is Poisson's ratio. From this, W_t and W_v can be calculated as:

$$W_t = \pi p^2 a^3 (1+\nu) / E \tag{15}$$

$$W_v = {}^2/_3 \, \pi p^2 a^3 / LSS \tag{16}$$

From W_t we can calculate LERR as:

$LERR = W_t / Volume$

$$= \pi p^2 a^3 (1+\nu) / E / ({}^4/_3 \, \pi a^3)$$

$$= {}^3/_4 \, p^2 (1+\nu) / E \tag{17}$$

By equating W_v to W_t, LSS can be determined as:

$$LSS = {}^2/_3 \, E / (1+\nu) \tag{18}$$

Note that this result is independent of the stress level and excavation size. This LSS is also approximately equal to the bulk modulus:

$$E / (3(1-2\nu)) \tag{19}$$

When $\nu = 0.25$

5.2 Verification for a pillar between two drives

Now reconsider the simple example of a pillar between two drifts run with different far field stress states (Figure 4). Recall that previously we calculated that LERR increased by a factor of four due to doubling of the stress state. If we now calculate LSS we find that it has the same value regardless of the stress state. This is exactly the result we wanted to achieve as we now have a parameter that is independent of the stress level (Figure 7).

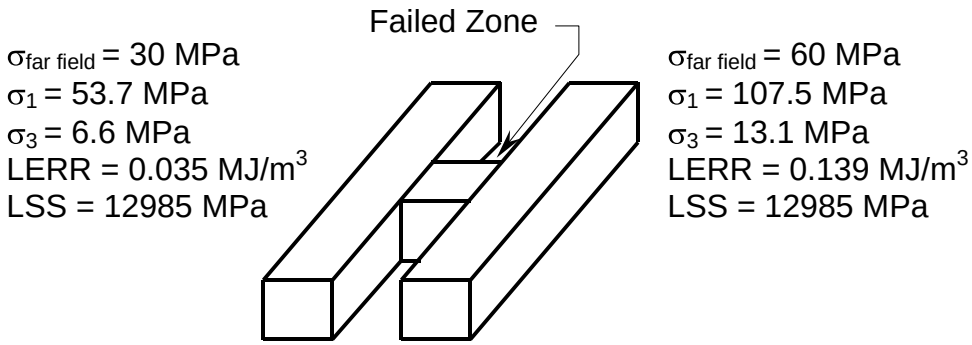

Figure 7 Pillar failure with different far field stress states (LSS added)

5.3 Verification for an abutment adjacent to a large stope

Now reconsider the example of mining adjacent to a large stope (Figure 5).

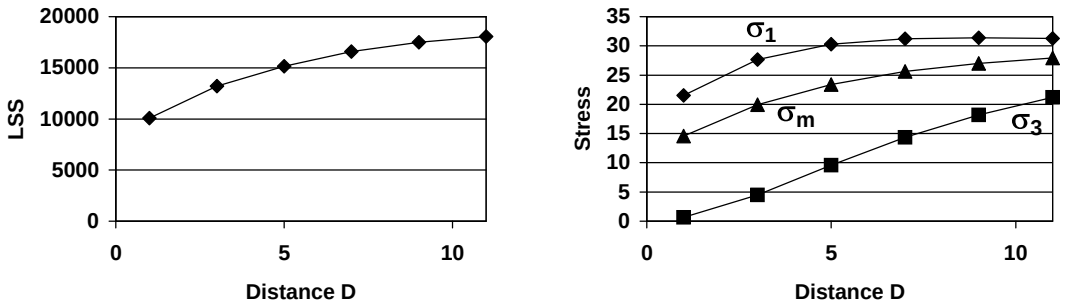

Figure 8 LSS and stresses near a large stope

Recall that LERR increases as we move away from the stope. If we now calculate LSS we get the expected response; LSS increases (indicating a decreasing potential for rockbursting) as we move away from the stope (Figure 8).

Finally, reconsider the Creighton back-analyses.

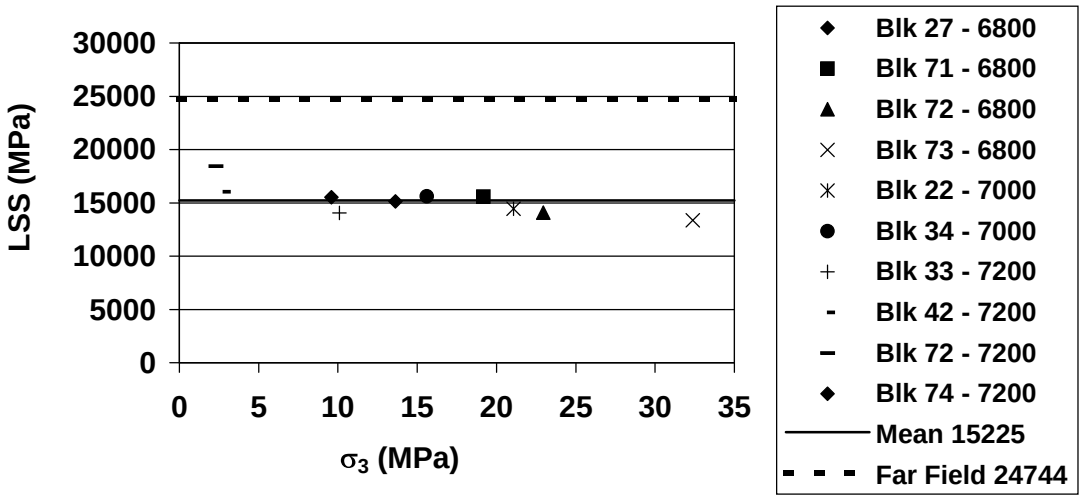

Figure 9 Local energy release rate at time of burst

It can be observed here (Figure 9) that LSS correlates very well with observed bursting (Cv ≈ 9%), in fact better than LERR (which has a Cv ≈ 14%).

5.4 Verification for Creighton mine

Now we shall look at some back-analysis results from Creighton mine to see what some LSS predictions look like for a real mining situation.

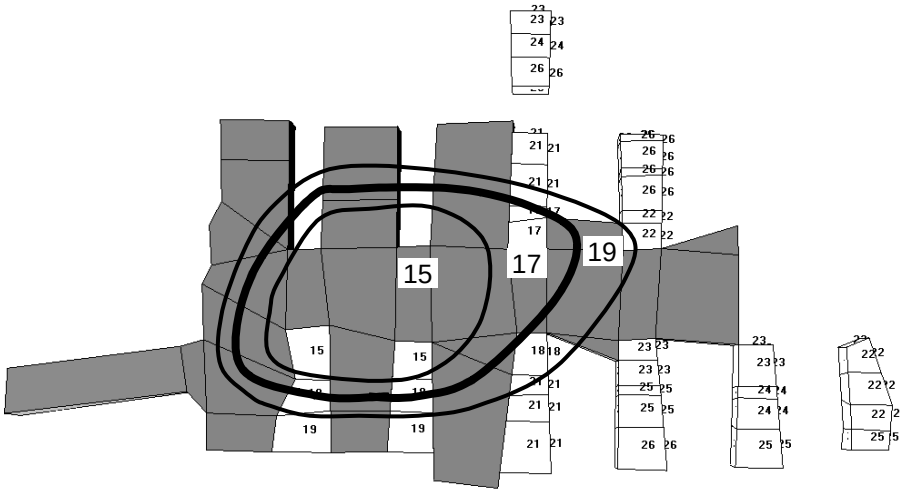

Figure 10 Loading system stiffness (LSS/1000 MPa) 7000 level mining step 3

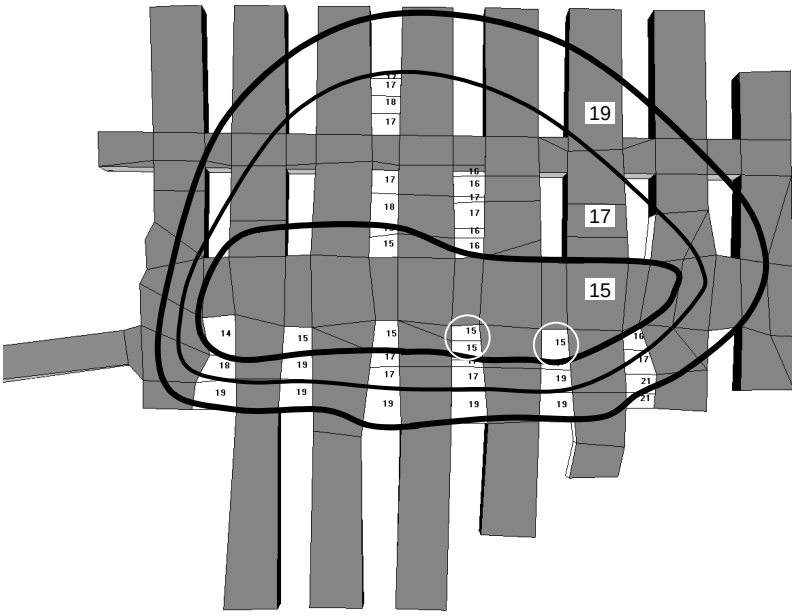

Figure 11 Loading system stiffness (LSS/1000 MPa) 7000 level mining step 7

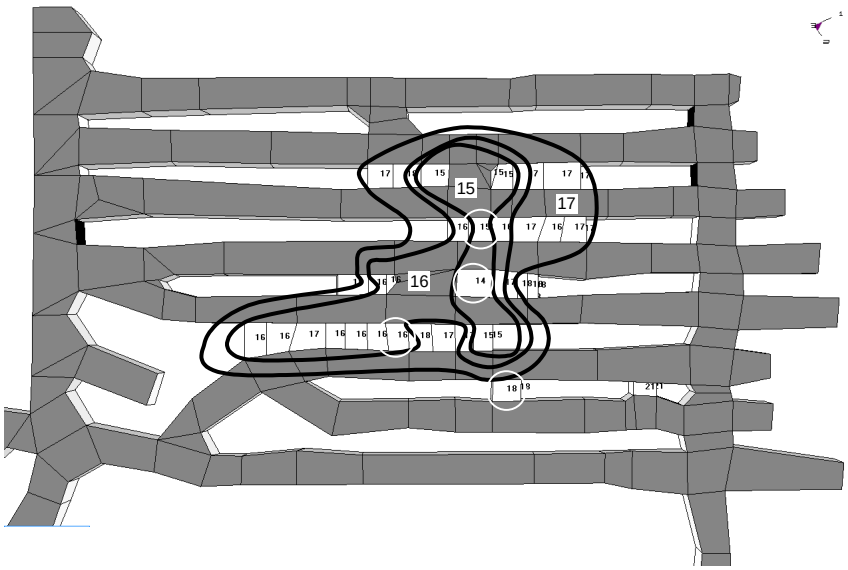

Figure 12 Loading system stiffness (LSS/1000 MPa) 7200 level mining step 6

In Figures 10, 11 and 12, the mining is shown in gray. The LSS has been calculated for a number of anticipated pillar failures (these blocks are labelled with their respective LSS values divided by 1000). Contour lines have been drawn through the LSS blocks to delineate zones of varying burst proneness. Noting that the critical value of LSS is 15225 MPa (see Figure 9), these results indicate that the pillars inside the contour labelled 15 are most prone to bursting. Indeed, almost all of the bursts (reported burst locations are circled in white) occurred within this contour. Burst proneness appears to decrease as you move away from this inner zone towards the extremities of mining. Additional pillar failures should be tested, to refine these contours and identify any local hotspots that may exist.

The burst (lower right side of Figure 12) that plots outside of the contour labelled 15 can probably be explained by noting that this event occurred late in the mining sequence. Considerable convergence was noted on the level by this point in the mining sequence owing to the failure of many pillars and considerable ground conditioning induced by destress blasting. The elastic analysis used here does not account for any stress redistribution resulting from this convergence.

From the assessment presented in Figures 10, 11 and 12, locations that are rockburst prone are clearly identified. This provides the opportunity to take special ground support measures at an appropriate time in the mining sequence. Such measures (ground preconditioning) were in fact taken in these areas during mining.

6 Conclusion

Assessment of burst potential requires that two questions be answered:

- Is it likely that a failure will occur?
- If a failure were to occur, would it be violent or not?

It has been shown in previous work (Wiles, 1998) that the likelihood of failure can be reliably estimated by calibration of a strength envelope using back-analyses of observed failures.

Since the local energy release rate is heavily dependent on the local stress level, it can only be used to predict the expected nature of failure (violent or gentle) for stress states that are exactly at the point of failure (i.e. on the failure envelope). This makes this parameter unsuitable for prediction of burst proneness because whenever stress states are above or below the strength envelope, erroneously high or low values of are obtained. This invalidates predictions for the expected nature of failure based on local energy release rate.

A representative measure of loading system stiffness can be obtained by normalising the local energy release rate by the square of the mean stress. This eliminates dependence on the local stress level and provides an indicator that can be used to predict the expected nature of failure regardless of whether the stress state is exactly at the point of failure.

Loading system stiffness can therefore be used to determine the likelihood that a failure will be violent. This provides a technique to identify locations that are rockburst prone, thus providing the opportunity to take special ground support measures at an appropriate time in the mining sequence.

Acknowledgements

Many thanks to INCO Ltd. for providing the data used in the case studies.

References

Barenblatt, G.I. (1962) The mathematical theory of equilibrium cracks in brittle fracture, advances in applied mechanics, Vol. 7, pp. 55–129.

Griffith, A.A. (1921) The phenomena of rupture and flow in solids, Phil. Trans. Royal Society London, Series A, Vol. 221, pp. 163–198; and then (1924) Proceedings International Congress of Applied Mechanics, Delft, The Netherlands, pp. 55–63.

Timoshenko, S.P. and J.N., Goodier (1934) Theory of Elasticity. McGraw-Hill Book Company, New York, 567 p.

Wiles, T.D. (1998) Correlation between local energy release density and observed bursting conditions at Creighton mine, Mine Modelling Ltd, Sudbury, 88 p.